Available online at www.sciencedirect.com

ScienceDirect

Polymer 48 (2007) 5417–5430

polymer

www.elsevier.com/locate/polymer

Mixed matrix membranes of sodium alginate and poly(vinyl alcohol) for pervaporation dehydration of isopropanol at different temperatures☆

Susheelkumar G. Adoor, B. Prathab, Lata S. Manjeshwar, Tejraj M. Aminabhavi*

Membrane Separations and Molecular Modeling Divisions, Center of Excellence in Polymer Science, Karnatak University, Dharwad 580 003, Karnataka, India

Received 13 December 2006; received in revised form 17 June 2007; accepted 27 June 2007
Available online 5 July 2007

Abstract

Mixed matrix membranes of sodium alginate (NaAlg) and poly(vinyl alcohol) (PVA) containing 5 and 10 wt.% silicalite-1 particles were fabricated by solution casting method and the cured membranes were crosslinked with glutaraldehyde. These membranes were used in pervaporation (PV) dehydration of isopropanol at 30, 40, 50 and 60 °C. Membrane morphology was studied by scanning electron microscopy and universal testing machine to assess their mechanical strengths. Swelling results of the pristine and mixed matrix membranes were correlated with their PV performances. Selectivities of the mixed matrix membranes of NaAlg were 11,241 and 17,991 with the fluxes of 0.039 and 0.027 kg/m^2 h, respectively, for 5 and 10 wt.% silicalite-1 loadings. Corresponding values for mixed matrix membranes of PVA were 1295 and 2241, and 0.084 and 0.069 kg/m^2 h, respectively, for 10 wt.% water-containing feed at 30 °C. Pristine membranes of NaAlg and PVA exhibited lower selectivities of 653 and 77 with increased fluxes of 0.067 and 0.095 kg/m^2 h, respectively. From the temperature dependence of flux and diffusivity data with 10 wt.% water-containing feed, Arrhenius plots were constructed to compute heat of sorption, ΔH_s values. Mixed matrix membranes of NaAlg were better than PVA mixed matrix membranes at all compositions (10–40 wt.%) of water. Molecular dynamics (MD) simulation was employed to compute the interfacial interaction energies of NaAlg and PVA polymers with silicalite-1 filler; also sorption of liquid molecules was computed. Simulated diffusivities compared well with the experimental data. Thermodynamic treatment of sorption, diffusion and permeation processes was attempted based on the Flory–Huggins theory to explain the PV performances of the membranes.

Keywords: Sodium alginate; Poly(vinyl alcohol); Silicalite-1

1. Introduction

Pervaporation (PV) has been regarded as an energy intensive technique that has been successfully used to dehydrate organic solvents [1]. In PV, the liquid feed mixture is maintained at the upstream side of the membrane, while permeate is removed in a vapor form by application of vacuum on the downstream side. The vapor is condensed using liquid nitrogen. In view of its simplicity, low costs, reasonable flux and high selectivity, PV is a popular membrane-based dehydration technique for various organics [2] as well as in separating azeotropes, isomers and heat sensitive compounds, whose separations cannot be easily achieved by other conventional means like distillation [3,4].

In our continuing efforts on PV dehydration of organics, the present study deals with a comparison of the PV performance of mixed matrix membranes of sodium alginate (NaAlg) and poly(vinyl alcohol), PVA by adding silicalite-1 particles in two different ratios (5 and 10 wt.%). NaAlg is a well-known water-soluble polysaccharide, having good membrane forming properties, which could be crosslinked with glutaraldehyde or Ca^{2+} ions [5] and its performance was found to be better than PVA [6], ion-exchange resins [7] and some other polysaccharides such as chitosan [8] and cellulose [9]. PVA has also been widely used as a membrane in PV dehydration of organics due to its hydrophilic nature, good film forming property and chemical resistivity [10,11]. Its excessive swelling in the

---

☆ This paper is Center of Excellence in Polymer Science communication # 149.

* Corresponding author. Tel.: +91 836 2215372; fax: +91 836 2771275.
E-mail address: aminabhavi@yahoo.com (T.M. Aminabhavi).

0032-3861/$ - see front matter © 2007 Elsevier Ltd. All rights reserved.
doi:10.1016/j.polymer.2007.06.064

Nomenclature

J, J_{i} and J_{j}	Total flux, water flux and isopropanol flux (kg/m h)
C_{p}	Weight of liquids' permeated (kg)
A	Effective membrane area (m^2)
t	Time (h)
α	Selectivity
$W_{\mathrm{i,p}}$	Wt.% of water in the permeate
$W_{\mathrm{i,f}}$	Wt.% of water in the feed
D_{i}, D_{j} and D_{m}	Diffusion coefficients of water, isopropanol and water + isopropanol mixture (m^2/s)
$C_{\mathrm{i,m}}$, $C_{\mathrm{i,f}}$ and $C_{\mathrm{i,p}}$	Local water concentrations in membrane, feed, and permeate (g/cm^3) at the position coordinate z
Q_{i}	Specific permeation rate of water (g/m^2 h)
$C_{\mathrm{i,f,m}}$ and $C_{\mathrm{i,p,m}}$	Concentrations of water (g/cm^3) at the membrane surface of the feed side (f) and permeate side (p)
δ	Maximum membrane thickness (μm)
K_{i}, K_{j} and K_{m}	Distribution coefficients of water, isopropanol and water + isopropanol mixture
P_{i}, P_{j} and P_{m}	Permeation coefficients of water, isopropanol and water + isopropanol mixture (m^2/s)
α_{perm}	Permselectivity
S_{d}	Relative ability of penetrants to pass through the membrane by diffusion
S_{k}	Relative affinity of penetrants to polymer
ρ_{m}	Membrane density (kg/m^3)
$D_{0,\mathrm{i}}$	Diffusion coefficient of water at infinite dilution (m^2/s)
m	Slope of water flux against wt.% of water in feed
h	Membrane thickness (μm)
φ_{i} and φ_{j}	Volume fractions of water and isopropanol in the swollen polymer membrane
v_{i} and v_{j}	Volume fractions of water and isopropanol in feed mixture
ρ_{P} and ρ_{S}	Densities of polymer and solvent
M_{b} and M_{a}	Weights of the membrane before and after swelling
x_{i} and x_{j}	Mole fractions of water and isopropanol
M_{i} and M_{j}	Molecular weights of water and isopropanol
ΔGE	Gibbs free energy of mixing (J/mol)
ρ_{sm}	Density of the solvent mixture
J_{p}	Permeation flux of water (kg/m^2 h)
J_{p0}	Permeation rate constant
E_{p}	Activation energy for permeation (kJ/mol)
R	Molar gas constant (J/K/mol)
T	Temperature (K)
D_0	Diffusion rate constant
E_{d}	Activation energy for diffusion (kJ/mol)
$r_i(0)$	Initial position coordinate of penetrant molecule in polymer microstructure
$r_i(t)$	Position coordinate of penetrant molecule after time, t
ΔH_{s}	Heat of sorption (kJ/mol)

presence of hydrophilic solvents was overcome by modifications such as blending [12], grafting [13], crosslinking [14], etc.

In recent years, mixed matrix membranes incorporated with zeolites or other inorganic fillers have been widely studied for PV dehydration of organics [15]. However, silicalite-1, a hydrophobic inorganic material, has been rarely used [16–18] as a filler to fabricate mixed matrix membranes. Silicalite-1 has a high Si/Al ratio, which makes it hydrophobic. It has an asymmetrical aperture with a three-dimensional channel system. The present study deals with investigations on the development of mixed matrix membranes of NaAlg and PVA containing silicalite-1 particles for applications in isopropanol dehydration, since the latter is an important and commercially used solvent in many industrial sectors. It is miscible with water in all proportions and forms an azeotrope at 12.5 wt.% of water. Its azeotrope is difficult to be separated by simple distillation and the process becomes more health hazardous as well as expensive than PV, as reported earlier [19].

PV results of the present study were further supported by molecular modeling (MM) approaches, leading to the understanding of polymer/non-polymer interfacial energies [20]. MD simulations were performed to investigate the interactions between polymers and silicalite-1 surfaces [21,22]. In addition, the liquid sorption phenomenon was studied through atomistic computations [23] to estimate the interaction energies of water and isopropanol with NaAlg and PVA matrices. The well-known Flory–Huggins theory was employed to understand such interactions to accomplish a better understanding of the PV dehydration process in terms of the thermodynamic parameters.

2. Experimental

2.1. Materials

Sodium alginate ($\overline{M}_{\mathrm{w}} = 122,594$), poly(vinyl alcohol) ($\overline{M}_{\mathrm{w}} = 125,000$), isopropanol, glutaraldehyde (GA) and hydrochloric acid (HCl) of Analytical Reagent (AR) grade samples were purchased from S.D. fine Chemicals, Mumbai, India; these were used as received. Deionized water having a conductivity of 20 μS/cm was produced in the laboratory itself from the Permeonics pilot plant (Vadodara, India) using the nanofiltration membrane module. Silicalite-1 zeolite was kindly supplied by Dr. S.B. Halligudi, National Chemical Laboratory, Pune, India.

2.2. Membrane fabrication

All the membranes were fabricated at ambient temperature (30 °C). NaAlg (4 g) was dissolved in 80 mL of water with constant stirring. Then, 0.2 and 0.4 g of silicalite-1 particles weighed separately were dispersed in 20 mL of water, sonicated for 2 h and added to the previously prepared NaAlg solution. The mixture was stirred for 24 h and poured onto a glass plate to cast the membranes. Dried membranes were peeled off from the glass plate and immersed in a crosslinking bath containing water/acetone (30/70) mixture along with 2 mL of GA and 2 mL of conc. HCl. Acetone, being a non-solvent, prevented the initial dissolution of the membrane and water present in the feed mixture caused membrane swelling, thereby facilitating an easy penetration of glutaraldehyde into the membrane matrix to establish an effective crosslinking. After allowing for 10 h, the crosslinked membranes were removed from the bath, washed repeatedly with deionized water and dried in an oven at 40 °C. Pristine NaAlg membrane was prepared by crosslinking with 2.5 mL of GA and 2.5 mL of conc. HCl for 10 h. Membrane thicknesses as measured by a micrometer screw gauge were 50 ± 1.0 μm. It was found that silicalite-1 loading had a significant influence on the uniformity of the membrane. The mixed matrix membranes were found to be homogeneous at 5 and 10 wt.% filler loadings, but non-uniform and brittle films were obtained at higher loadings of the filler and hence were not attempted. The fabricated membranes were designated as NaAlg-1 and NaAlg-2, respectively. The same procedure was followed for the fabrication and crosslinking of PVA mixed matrix membranes taking the same wt.% of silicalite-1 in PVA. These membranes were designated, respectively, as PVA-1 and PVA-2.

2.3. Scanning electron microscopy (SEM)

Typical SEM micrographs of NaAlg-2 and PVA-2 mixed matrix membranes were taken under high resolution (Mag. 300× at 5 kV) to study the distribution of silicalite-1 particles in both the membranes. Scanning was done using JOEL MODEL JSM 840A, Japan. Since these membranes were non-conductive gold coating (15 nm thickness) was done on the samples before injecting to SEM analysis.

2.4. Particle size measurement of silicalite-1

Zeta average diameter of silicalite-1 zeolite particles dispersed in water was measured by Zetasizer laser light scattering equipment (Model 3000HS, Malvern, Buntsford, United Kingdom).

2.5. Universal testing machine (UTM)

Tensile strength and % elongation at break of the pristine NaAlg, pristine PVA, NaAlg-1, NaAlg-2, PVA-1 and PVA-2 mixed matrix membranes were measured using universal testing machine (Model H 25 KS, Hounsfield, Surrey, United Kingdom). Test specimens were prepared in the form of dumbbell shapes as per ASTM D-638 standards. Films of gauge length of 50 mm and 10 mm width were stretched at the crosshead speed of 10 mm/min.

2.6. Pervaporation experiments

Pervaporation experiments were carried out as detailed before [24,25] on a 100 mL batch level instrument with an indigenously constructed manifold operated at a vacuum level as low as 0.05 mmHg in the permeate line. Effective membrane area was 20 cm^2 and weight of the feed mixture taken in the PV cell was 70 g. Temperature of the feed mixture was maintained constant by a thermostatic water jacket. In view of the concentration polarization effect, feed mixture was continuously stirred with an overhead stainless steel stirrer fitted with a Teflon edge at 60 rpm. Before starting the PV experiment, test membrane was equilibrated for 2–4 h with the feed mixture. After establishment of a steady state, permeate vapors were collected in cold traps immersed in liquid nitrogen up to 4–5 h. Weight of permeate collected was measured on a Mettler Balance (model B 204-S, Greifensee, Switzerland: accuracy 10^{-4} g) to determine the flux:

$$J = \frac{C_\mathrm{p}}{At} \tag{1}$$

The analysis of feed and permeate samples was done using gas chromatography (Nucon, model 5765, Mumbai, India) provided with a Thermal Conductivity Detector (TCD) equipped with a DEGS or Tenax packed column of 1/8″ ID having 2 m length. Oven temperature was maintained at 70 °C (isothermal), while injector and detector temperatures were maintained at 150 °C. The sample injection volume was 1 μL. Pure hydrogen was used as a carrier gas at a pressure of 0.75 $\mathrm{kg/cm}^2$. The GC response was calibrated for column and for known compositions of water + isopropanol mixtures. Calibration factors were fed into GC software to obtain the analysis for unknown samples. Then, selectivity, α was calculated as:

$$\alpha = \left[\frac{W_\mathrm{i,p}}{1 - W_\mathrm{i,p}}\right]\left[\frac{1 - W_\mathrm{i,f}}{W_\mathrm{i,f}}\right] \tag{2}$$

A minimum of three independent measurements of flux and α was taken under similar conditions of temperature and feed compositions to confirm the steady-state pervaporation. The same membrane was used for performing three independent measurements and the difference between these measurements was negligible. This shows that there is no chemical alteration in the membrane even after repeated cycles of PV operations, suggesting their sturdiness with respect to the chemical structure. These data were reproducible within ±3% of standard deviations, but the average values were considered in calculations and data display.

2.7. Degree of swelling

Equilibrium swelling experiments were performed gravimetrically [26] on all the membranes in 10, 20, 30 and 40 wt.% water-containing feed mixtures at 30 °C to calculate the % degree of swelling. Initial weight of the circularly cut (dia = 2.5 cm) pristine and mixed matrix membranes was taken on a single-pan digital microbalance (model AE 240, Mettler, Griefensee, Switzerland) sensitive to ±0.01 mg. Samples were placed inside the specially designed airtight test bottles containing 20 cm^3 of the test solvent. Test bottles were transferred to the oven maintained at the constant desired temperature. Dry membranes were equilibrated by soaking in different compositions of the feed mixtures in a sealed vessel at 30 °C for 48 h. The swollen membranes were weighed immediately (after careful blotting with soft tissue papers) on a digital microbalance. The % degree of swelling, DS was calculated as before [26]. Sorption selectivity experiments were also performed using the procedure described elsewhere [27].

3. Diffusion, sorption and permeation processes

Mass transfer in binary feed mixtures through non-porous dense membrane has been described by the solution–diffusion mechanism [28]. Penetrant migration is generally controlled by diffusion, since fast distribution equilibrium can be established between the bulk feed and the upstream surface of the membrane [29]. The local diffusion rate, J_i (or J_j) in a membrane can be described by the Fick's first law of diffusion [30], which under steady-state conditions, takes the following form for one-dimensional diffusion:

$$J_i = D_i(C_{i,m})\frac{dC_{i,m}}{dz} \tag{3}$$

where D_i is influenced by the solute concentration, but due to immobilization of the membrane, D_i can be regarded as self-diffusion coefficient and J_i is calculated per unit of the cross-sectional area of the membrane.

For a planar membrane, permeation rate, Q_i, can be calculated by integrating Eq. (3) from the upstream to downstream side across the membrane:

$$Q_i = \int_0^{\delta} J_i\,dz = \int_{C_{i,p,m}}^{C_{i,f,m}} D_i(C_{i,m})dC_{i,m} \tag{4}$$

Upon solving Eq. (4), we get:

$$Q_i = J_i\delta = D_i\left(C_{i,f,m} - C_{i,p,m}\right) \tag{5}$$

Under steady-state conditions, J_i is constant, but due to low downstream pressure, we have: $C_{i,p,m} \approx 0$ and $C_{i,p} \approx 0$ and hence, we can simplify Eq. (5) to give:

$$D_i = \frac{J_i\delta}{C_{i,f,m}} \tag{6}$$

Distribution coefficient, K_i and permeation coefficient, P_i are defined as:

$$K_i = \frac{C_{i,f,m}}{C_{i,f}} \tag{7}$$

$$P_i = \frac{Q_i}{C_{i,f} - C_{i,p}} \approx \frac{Q_i}{C_{i,f}} = \frac{J_i\delta}{C_{i,f}} \tag{8}$$

Then, by combining Eqs. (6)–(8), we get:

$$P_i = D_iK_i \tag{9}$$

If the vapor pressure difference is used to substitute liquid concentration difference as the driving force for permeation [31], then it is possible to describe the dependence of P_i and D_i on temperature with the Arrhenius relationship. Hence, permselectivity of a membrane is defined as [32]:

$$\alpha_{perm} = \frac{P_i}{P_j}\frac{D_i}{D_j}\frac{K_i}{K_j} = S_dS_k \tag{10}$$

where

$$S_d = \frac{D_i}{D_j} \text{ and } S_k = \frac{K_i}{K_j} \tag{11}$$

Considering that the presently developed hydrophilic membranes incorporated with a hydrophobic silicalite-1 particles exhibit high affinity towards water and hence, diffusion coefficient is dependent upon water concentration of the feed, then there will not be any coupling effect such that water flux can be calculated as [33]:

$$J_i = \frac{\rho_m D_{0,i}\left(K_iW_{i,f}\right)^m}{mh} \tag{12}$$

The observed differences in selectivity can be explained by the thermodynamic treatment given by Aminabhavi and Munk [34], who modified the original Flory–Huggins theory for a three-component system to compute the preferential interaction of polymers in a mixed solvent system by calculating the Gibbs free energy of mixing (ΔG_{mix}). Later, Mulder and Smolders [35] have extended this concept to PV phenomenon. Thus, we have:

$$\begin{aligned} \ln\alpha_S &= \ln\left(\frac{\varphi_i}{\varphi_j}\right) - \ln\left(\frac{v_i}{v_j}\right) \\ &= \left(\frac{V_i}{V_j} - 1\right)\ln\left(\frac{\varphi_j}{v_j}\right) - \chi_{ij}\left(\varphi_j - \varphi_i\right) - \chi_{ij}\left(v_i - v_j\right) \\ &\quad - \phi_P\left(\chi_{iP} - \frac{V_i}{V_j}\chi_{jP}\right) \end{aligned} \tag{13}$$

The values of molar volume, V at 30 °C for water and isopropanol were taken from the literature [36]. The volume fraction, ϕ_P, of the polymer in the swollen state was calculated using [37]:

$$\phi_P = \left[1 + \frac{\rho_P}{\rho_S}\left(\frac{M_a}{M_b}\right) - \left(\frac{\rho_P}{\rho_S}\right)\right]^{-1} \tag{14}$$

Molar volume of the binary mixtures of water–isopropanol was calculated as:

$$V = \frac{\left(x_iM_i + x_jM_j\right)}{\rho_{sm}} \tag{15}$$

The interaction parameter, χ_{ij} between water and isopropanol was calculated using the equation [38]:

$$\chi_{ij} = \frac{\left[x_i\ln(x_i/v_i) + x_j\ln(x_j/v_j) + \left(\Delta G^E/RT\right)\right]}{x_iv_j} \tag{16}$$

Excess Gibbs free energy, ΔG^{E} was calculated using the activity coefficients, γ of the mixtures as:

$$\Delta G^{\mathrm{E}} = RT\left(x_{\mathrm{i}} \ln \gamma_{\mathrm{i}} + x_{\mathrm{j}} \ln \gamma_{\mathrm{j}}\right) \tag{17}$$

In the absence of any direct experimental data on γ_{i} and γ_{j}, we have used the van Laar equation at 30 °C to compute the activity coefficient, γ_{i} of component, i in the mixture as:

$$\ln \gamma_{\mathrm{i}} = A_{\mathrm{ij}} = \left(\frac{A_{\mathrm{ij}} x_{\mathrm{j}}}{A_{\mathrm{ij}} x_{\mathrm{i}} + A_{\mathrm{ij}} x_{\mathrm{j}}}\right)^2 \tag{18}$$

The van Laar parameters, A_{ij} for water and A_{ji} for isopropanol were taken from the literature [39]. Then, the polymer–solvent interaction parameter, χ_{iP} was calculated from the Flory–Higgins equation [40]:

$$\chi_{iP} = \frac{V_i(\delta_P - \delta_i)^2}{RT} \tag{19}$$

Solubility parameters of NaAlg, PVA, water and isopropanol were, respectively, taken as 61.48, 52.67, 97.8 and 41.8 $(\mathrm{J/cm^3})^{1/2}$. These data were fitted into Eq. (13) to compute sorption selectivity, α_{S}. Crosslinking agent glutaraldehyde and the filler, silicalite-1 were not considered in Eq. (13), since their amounts are very small compared to polymers and solvents. These terms in Eq. (13) were negligible compared to the other terms, making no drastic changes in the results of theoretical sorption selectivity values [27]. Also, silicalite-1 is not soluble in any solvents but it is only dispersed. Therefore, the solubility parameter for silicalite-1 cannot be calculated; however, the changes observed in experimental results of the mixed matrix membranes are due to the surface adsorption capacity of the silicalite-1. Experimental and calculated sorption selectivity values are compared in Table 1. In all the cases, the calculated values are smaller than the experimental data.

Table 1
Sorption selectivity of different membranes for water–isopropanol mixture at 30 °C

Wt.% of water in feed	Sorption selectivity (expt.)	Sorption selectivity (calc)
NaAlg		
10	110	100
15	50	40
20	35	30
30	20	15
40	10	6
NaAlg-1		
10	1020	930
15	660	647
20	415	400
30	110	102
40	30	24
NaAlg-2		
10	1450	1414
15	600	584
20	535	521
30	130	122
40	68	55
PVA		
10	40	35
15	30	24
20	21	15
30	15	10
40	6	4
PVA-1		
10	400	383
15	185	175
20	130	120
30	60	54
40	25	17
PVA-2		
10	610	601
15	240	232
20	160	150
30	70	63
40	25	18

3.1. Estimation of interaction energies

MD simulations were performed to estimate the interaction energies between polymers and solvents in addition to silicalite-1 particles. The COMPASS (condensed-phase optimized molecular potentials for atomistic simulation studies) forcefield [41,42] was used, wherein oligomer chain of the chosen polymer was generated in an *isotactic* configuration taking 20 monomer units and was minimized to construct the amorphous cells based on the respective densities of the selected oligomers of each polymers. Details of the construction of amorphous cell module were reported earlier [43]. The cell dimensions were taken such that a and b (crystal) lattice parameters for the oligomer remained the same as the u and v (surface) parameters for silicalite-1 surface. The unit cell structure of silicalite-1 was generated using the surface builder module of MS modeling by employing the desired cleave planes ($h\ k\ l$), which provide the fractional depth of the surface that should be more than the non-bonded cut-off distance of 9.5 Å. After completing the energy minimization using steepest descent and conjugate gradient method, surface structure was converted into a non-periodic superstructure for use in crystal surface building step.

Crystal surface of silicalite-1 slab to be used in the simulation box to calculate the surface energy was built by the crystal builder implemented in MS modeling. The oligomers of NaAlg and PVA polymers were assembled into the simulation box with silicalite-1 surface. The c-dimension of the box was extended to 30 Å such that the oligomer was at an equidistance from the silicalite-1 surface. MD simulation was performed for 100,000 steps with a time step of 1 fs at 303 K. As the silicalite-1 surface was minimized in the earlier step, the entire surface atoms were constrained during the NVT dynamics. The energy of interaction was then calculated using Eq. (20). At first, the energy (E_{total}) for the simulation box containing NaAlg and PVA polymers with the surface atoms was calculated. Then, the energy of oligomers (E_{oligomer}) was calculated without any contribution from the surface. Finally, surface atoms were kept constant and oligomers were removed to calculate the surface energy (E_{surface}). The interaction energy of oligomers and surfaces was computed using:

$$E_{\text{interaction}} = E_{\text{total}} - \left(E_{\text{surface}} + E_{\text{oligomer}}\right) \tag{20}$$

Polymer–solvent interactions have been estimated using the MD simulations. NaAlg and PVA oligomeric slabs were constructed using the confined layer (cell type) dialog in the amorphous builder. As a part of the amorphous cell construction, a geometry refinement of the structure was performed. Further, two-dimensional boxes were built using the algorithm as described before; then, NaAlg and PVA as well as the selected fluid slabs were piled up and the box was extended by 100 Å in the *c*-direction. In order to pile the cells correctly, solvent layers (for 100 molecules of water layer) were selected with the same base to be compatible with those of NaAlg and PVA. MD simulations were run in the NVT ensemble at 303 K with tail correction being applied outside the cutoff of 9.5 Å. This ensured that a relatively thin layer would feel the effective pressure equivalent to that in the bulk. The systems were then allowed to equilibrate normally against vacuum for approximately 30,000 steps. This was followed by 300 ps of the MD run. For every 500 fs, the energy of interaction between oligomers and liquid layer was evaluated using 18 Å cut-off distance without the tail correction. A total of 600 energy calculations were performed for each system (300 ps was the total simulation time).

3.2. Computation of diffusion coefficients

Diffusion coefficients of water and isopropanol in NaAlg and PVA were calculated by a modification of the established protocols for polymers [44,45]. The construction methodology remained the same as described before. NaAlg and PVA structures were generated with six polymer chains and each polymer chain was built from 10 repeat units. Different mixture compositions of 10, 15, 20, 30, 40 and 50 wt.% water and remaining isopropanol molecules were placed in the same cell. The length of sides of cubic unit cells was chosen between 17.94 and 22.78 Å. After generating the initial structures, MD simulations under NVT ensemble were performed at 303 K for each configuration in which all the interactions were considered. Minimization was performed using the same algorithms as mentioned before. Equilibration run up to 200 ps was performed with the NVT ensemble. However, for the production run, it is best to switch to NVE ensemble, but depending upon the thermostatting method used, NVE dynamics did not artificially interfere with the thermodynamics of the system. Hence, a simulation time of 200 ps of NVE ensemble was applied.

Diffusion coefficients of water and isopropanol at 300 K in the equilibrated structures of NaAlg and PVA were determined using the mean-square displacements (MSD) of the molecules as per Einstein's equation:

$$D = \frac{1}{6N_\alpha} \lim_{t\to\infty} \frac{\mathrm{d}}{\mathrm{d}t} \sum_{i=1}^{N_\alpha} \left\langle [r_i(t) - r_i(0)]^2 \right\rangle \tag{21}$$

Here, $[r_i(t) - r_i(0)]$ represents the displacement of the penetrant molecule during time, *t*. Diffusion coefficient, *D* remains constant, i.e., independent of penetrant concentration in the polymer. The MSD, i.e., $\{[r_i(t) - r_i(0)]^2\}$ for water and isopropanol were calculated from 200 ps trajectories of the molecules in NaAlg and PVA. According to Eq. (21), the plot of MSD vs time should be strictly linear if *D* remains constant, i.e., if the molecule exhibits normal (Einstein) diffusion behavior. It is, however, observed that plots of MSD vs time (in ps) are indeed linear for the penetrant liquid molecules up to 170 ps. At longer times, these plots deviated slightly from the linearity due to increasing statistical errors involved in the MD simulations of MSD. All the *D* values were determined from the slopes of such plots using Eq. (21).

4. Results and discussion

4.1. Membrane morphology

Fig. 1 displays the surface SEM pictures of NaAlg-2 and PVA-2 mixed matrix membranes, wherein one can observe

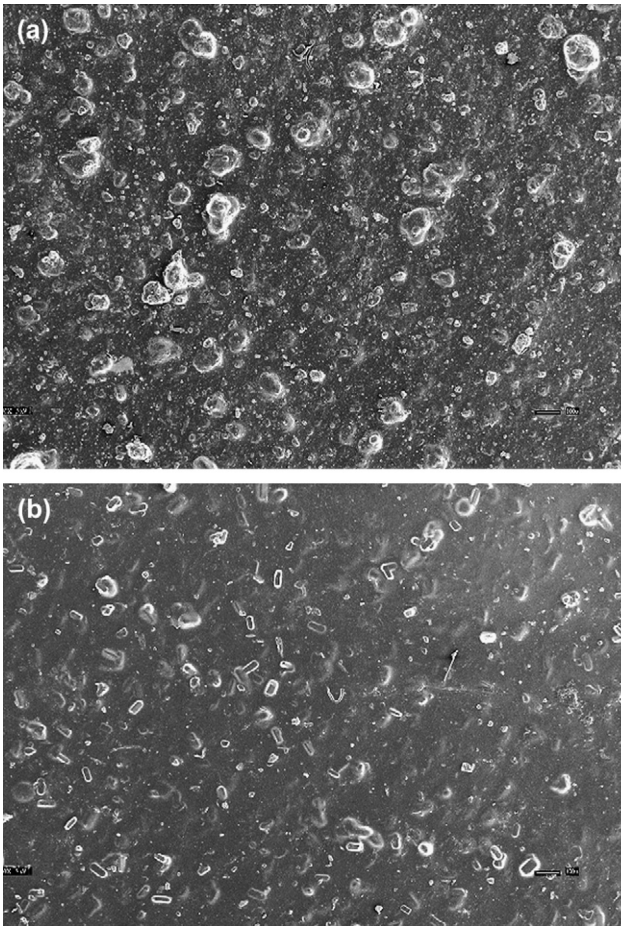

Fig. 1. SEM micrograph of (a) NaAlg-2 and (b) PVA-2 mixed matrix membranes.

the uniform distribution of silicalite-1 particles throughout the matrix; this would help to facilitate an easy transport of hydrophilic water molecules through the membranes.

4.2. Particle size measurement

The particle size distribution histogram of the silicalite-1 particles, not displayed to avoid too many figures, suggested that silicalite-1 particles have diameters that vary in the range of 0.8–0.9 μm.

4.3. Universal testing machine

Pristine NaAlg has the % elongation of 210 with a maximum tensile strength of 20 N/mm^2, whereas for NaAlg-1 and NaAlg-2 membranes, % elongations were 144 and 128 with the tensile strength values of 27 and 36 N/mm^2, respectively. The % elongation of pristine PVA was 269 with a maximum tensile strength of 30 N/mm^2, whereas for PVA-1 and PVA-2 membranes, % elongations were 180 and 155, while tensile strengths were 35 and 40 N/mm^2, respectively. These data clearly indicate that mechanical strengths of the mixed matrix membranes are better than those of the pristine membranes, suggesting their physical sturdiness.

4.4. Swelling

Fig. 2 shows the % degree of swelling of all the membranes at 30 °C performed in 10–40 wt.% of water-containing feed mixtures. Membrane swelling showed an influence on flux and selectivity. Pristine PVA was swollen more in water–isopropanol feed than in pristine NaAlg membrane, because of its linear structure. Therefore, the availability of –OH groups for an easy interaction with –OH groups of water and isopropanol will be more, signifying higher hydrophilic–hydrophilic interaction between PVA and water as compared to NaAlg and water. This has resulted in a higher flux of pristine PVA than pristine NaAlg membrane; consequently, the selectivity of pristine PVA is much smaller than pristine NaAlg membrane. Swelling of NaAlg/silicalite-1 and PVA/silicalite-1 mixed matrix membranes is lower than the respective pristine membranes. Since adsorption of silicalite-1 particles in NaAlg chain segments is higher than that of PVA, this would suppress the swelling of NaAlg more than that of PVA. But, due to the presence of higher number of hydroxyl groups in PVA compared to NaAlg, a decrease in swelling is not significant compared to NaAlg. As shown in Fig. 2, the observed swelling values in pristine NaAlg and PVA membranes are higher than those of the mixed matrix membranes due to the presence of silicalite-1 particles occupying the free volume spaces.

4.5. Membrane performance

Membrane performances of the pristine and mixed matrix membranes were studied in terms of flux, selectivity, diffusion coefficient, distribution coefficient, permeation coefficient and permselectivity.

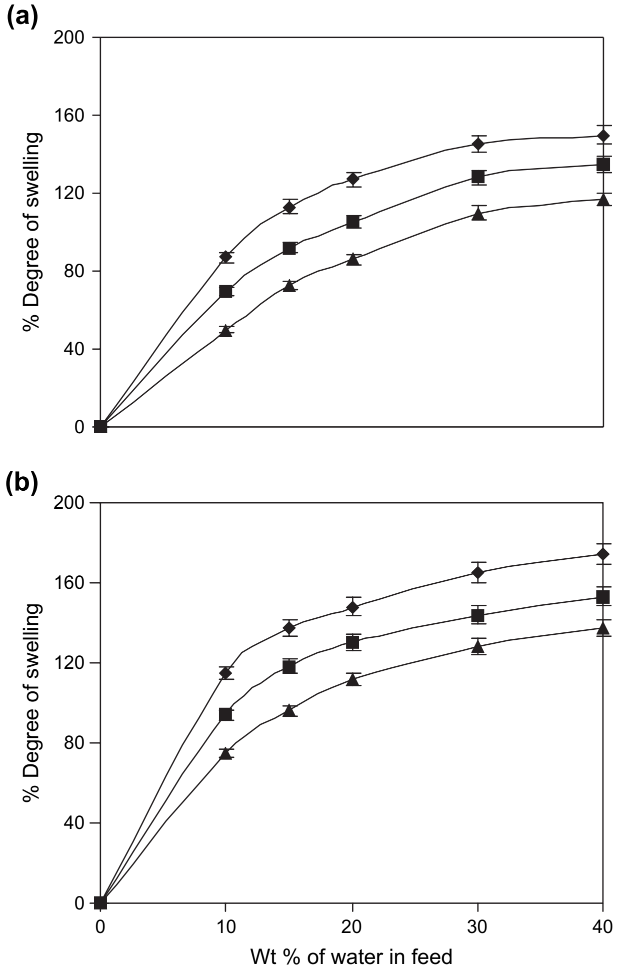

Fig. 2. Swelling curves of (a) pristine NaAlg (◆), NaAlg-1 (■) and NaAlg-2 (▲) membranes and (b) pristine PVA (◆), PVA-1 (■) and PVA-2 (▲) membranes.

4.5.1. Effect of silicalite-1 on membrane characteristics

The effect of silicalite-1 content on flux and selectivity of membranes at 30 °C is displayed in Fig. 3. Pristine NaAlg has a flux of 0.067 kg/m^2 h with a selectivity of 653, whereas pristine PVA has an increased flux of 0.095 kg/m^2 h with a lower selectivity of 77 for 10 wt.% water-containing feed. After incorporating silicalite-1 into PVA and NaAlg polymer matrices, the intrinsic properties of the membranes have changed and the selectivities of both pristine NaAlg and PVA membranes increased, but the flux values decreased. For instance, NaAlg-1 membrane exhibited a selectivity of 11,241, but for NaAlg-2 membrane, it was increased to 17,991 at 10 wt.% loading of silicalite-1 particles. In the case of PVA-1 and PVA-2 membranes, selectivity values were 1295 and 2241, respectively; these data are much lower than those of NaAlg-1 and NaAlg-2 membranes. For NaAlg-1 and NaAlg-2 membranes, fluxes are, respectively, 0.039 and 0.027 kg/m^2 h, whereas for PVA-1 and PVA-2 membranes, the corresponding flux values are 0.080 and 0.069 kg/m^2 h.

Even though both NaAlg and PVA polymers are hydrophilic, NaAlg could dehydrate isopropanol better than PVA

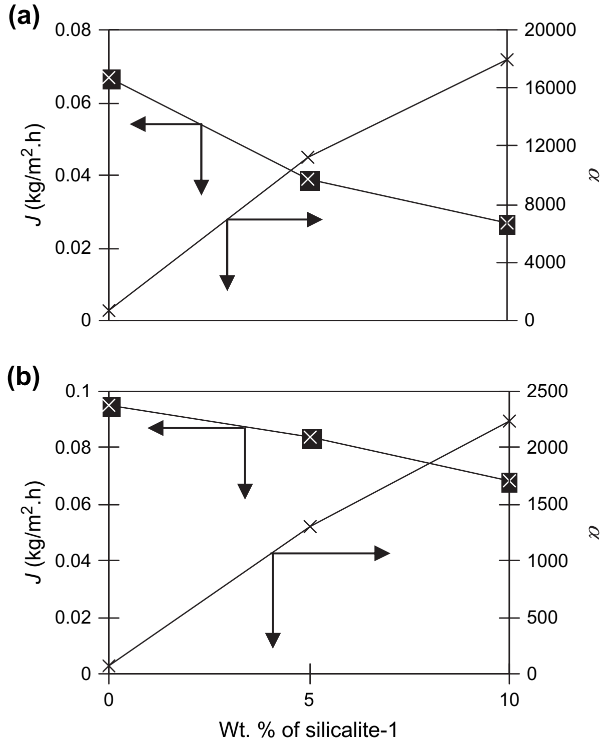

Fig. 3. Water flux and selectivity vs wt.% of silicalite-1 in (a) NaAlg and (b) PVA membranes for 10 wt.% water in the feed at 30 °C.

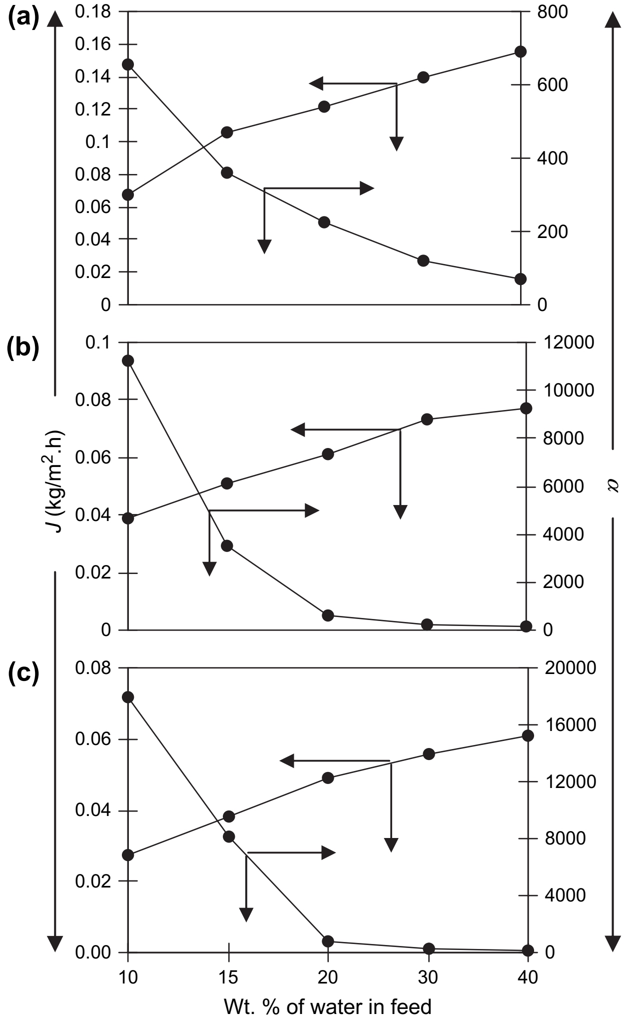

Fig. 4. Water flux and selectivity vs wt.% of water for (a) pristine NaAlg, (b) NaAlg-1 and (c) NaAlg-2 mixed matrix membranes for water + isopropanol feed mixtures at 30 °C.

as evidenced by higher selectivities due to difference in their swelling in the presence of hydrophilic solvents. Silicalite-1 being hydrophobic, its interaction with hydrophilic membranes and water are very important factors in PV separation. Silicalite-1 zeolite being hydrophobic could help to reduce the hydrophilicity of NaAlg as well as PVA membranes giving a decreased membrane swelling in the presence of water. It was reported before that hydrophobic–hydrophilic nature of zeolites also depends upon their framework structures [46]. Silicalite-1 possesses intricate three-dimensional sinusoidal channels [47], which would help to discriminate between the competing liquid molecules viz., isopropanol and water on the basis of molecular size difference as well as the polarity effect that could possibly influence the transport of water molecules through the mixed matrix membranes. However, the localized electrostatic forces between the positively charged cations and the negatively charged zeolitic framework strongly attract the highly polar water molecules than isopropanol as can be seen from the flux and selectivity results of NaAlg and PVA membranes presented at 30 °C in Figs. 4 and 5, respectively.

Membrane performance has been explained on the basis of solution–diffusion theory [27] as well as the adsorption–diffusion–desorption concepts [48] in mixed matrix membranes. In the case of pristine NaAlg and PVA membranes, the permeating water molecules get sorbed into the microvoids and then diffuse out on permeate side due to the existing concentration gradient. In the case of mixed matrix membranes, the overall separation can be explained by the hydrophilic–hydrophobic interactions between silicalite-1 and the polymers. The presence of silanol groups on silicalite-1 surfaces stemming from the intracrystalline boundaries and defects (or the lesser aluminum content present) could increase the local attraction towards water molecules, thereby making it more selective to water than isopropanol.

4.5.2. Effect of feed water composition on pervaporation performance

Figs. 4 and 5 display the effect of feed water composition on PV results of NaAlg and PVA membranes, respectively. As noticed before, pristine NaAlg and PVA membranes were swollen to a greater extent at high concentration of water, suggesting that both NaAlg and PVA membranes are mechanically somewhat weaker than the mixed matrix membranes. In the present investigation, it is demonstrated that by incorporating hydrophobic silicalite-1 particles, the solvent stability of PVA and NaAlg membranes has improved thus, facilitating the membrane performance. For both the mixed matrix membranes of NaAlg and PVA, flux has increased with increasing water concentration from 10 to 40 wt.% of the feed mixtures. At lower

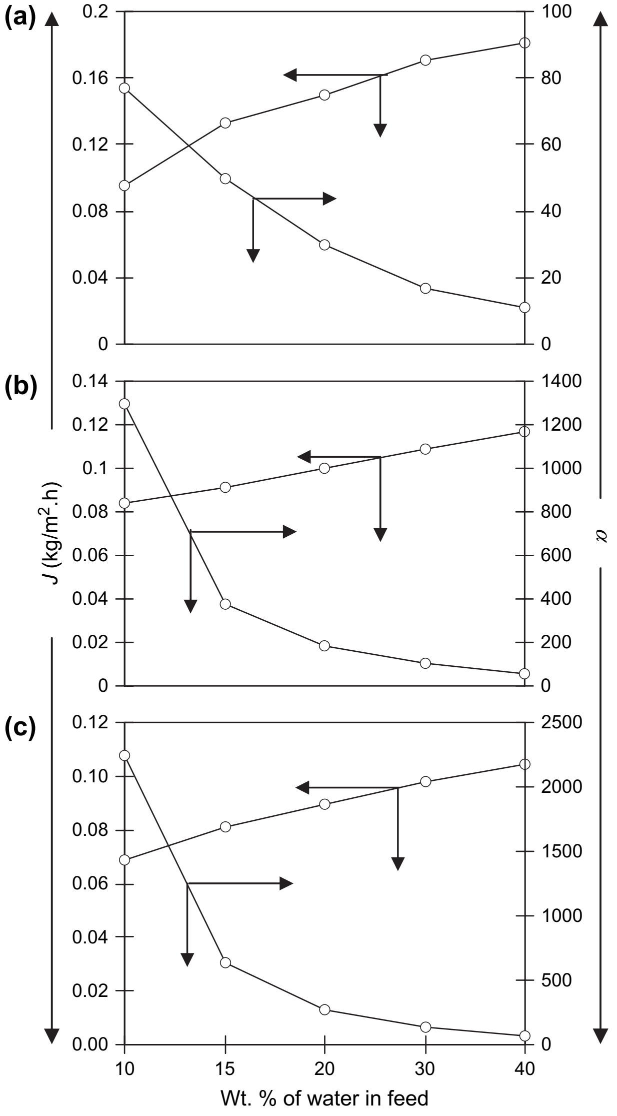

Fig. 5. Water flux and selectivity vs wt.% of water for (a) pristine PVA, (b) PVA-1 and (c) PVA-2 mixed matrix membranes for water + isopropanol feed mixtures at 30 °C.

water content of the feed mixture (10 wt.%), NaAlg-1, NaAlg-2, PVA-1 and PVA-2 membranes were swollen to a lesser extent due to the presence of hydrophobic silicalite-1 particles, which has reduced the excessive hydrophilic–hydrophilic interaction between hydroxyl groups of the membranes and water molecules. Any increase in water composition of the feed mixture will further decrease the selectivity to water quite considerably by increasing the flux value due to higher swelling of the membranes. The present mixed matrix membranes were able to withstand the cyclic PV operations even at higher water compositions of the feed without any cracks. This suggests that there is no breakage of ether linkages between PVA and glutaraldehyde as well as NaAlg and glutaraldehyde. Thus, the present membranes are chemically stable at all water compositions of the feed mixture.

At higher water composition of the feed mixture (40 wt.%), selectivities of NaAlg-1 and NaAlg-2 were dropped to as low as 125 and 163, but fluxes increased to 0.084 and 0.071 kg/m^2 h, respectively. In the case of PVA-1 and PVA-2 membranes, selectivity values were 59 and 72 with fluxes of 0.119 and 0.109 kg/m^2 h, respectively. For the same composition (40 wt.%) of water in the feed, pristine NaAlg had a selectivity of 72 with a flux of 0.155 kg/m^2 h, but for pristine PVA, a selectivity of 11 and a flux of 0.181 kg/m^2 h were observed. At higher water composition in the feed, polymer chain segments would follow a non-ordered trend, which may block the tortuous paths created by the silicalite-1 particles due to excessive swelling. This induces plasticization effect in the polymer chain segments, creating easy leaks for isopropanol molecules to transport through. Thus, for both the membranes, their performances varied depending upon the composition of water in the feed.

4.5.3. Effect of temperature

4.5.3.1. Acivation energy values. The PV membrane performance was tested at four temperatures viz., 30, 40, 50 and 60 °C, typically using 10 wt.% water-containing feed mixture. Membranes were stable at all these selected temperatures; flux and selectivity values were computed at all the temperatures. The operating temperature influences both the membrane intrinsic property and the driving force for penetrant transport through the membrane during pervaporation process. Membranes were found to be physically and chemically strong enough even at these elevated temperatures. As expected, the flux increased with increasing temperature, but selectivity decreased. The temperature dependency of flux was analyzed by Arrhenius equation of the type:

$$J_{\mathrm{P}} = J_{\mathrm{P}_0}\exp\left(-E_{\mathrm{p}}/RT\right) \tag{22}$$

If activation energy is positive, then permeation flux increases with increasing temperature, which has been observed in majority of PV experiments [27,49]. According to free volume theory [50], an increase in temperature increases thermal mobility of the polymer chains, which further generates extra free volume within the polymer matrix thereby, increasing the sorption and diffusion rates of permeant molecules. This type of increase in free volume of the membrane matrix will result in an easy transport of organic component of the mixed media. Consequently, the membrane selectivity to water will be reduced, but flux will be increased.

The driving force for permeation represents the concentration gradient, resulting from the difference in partial vapor pressure of the permeants between feed and permeate mixtures. As the feed temperature increases, vapor pressure in the feed compartment increases, but vapor pressure at permeate side is not affected. This would result in an increase of driving force with increasing temperature. The driving force is closely related to the phase transition in PV process and thus, is strongly dependent upon the operating temperature. This has affected the membrane performance in such a way that the flux was increased, but selectivity decreased with an increase in temperature.

Arrhenius plots of $\ln J_p$ vs $1/T$ are not displayed to avoid overcrowding of plots, but the calculated E_p values for pristine NaAlg, NaAlg-1, NaAlg-2 membranes are, respectively, 18.5, 20.27 and 24.88 kJ/mol, indicating a gradual increase with increasing amount of silicalite-1; this is due to the difficulty in liquid transport to crossover the Eyring's energy barrier. In the case of PVA, PVA-1 and PVA-2 membranes, similar trends were observed, but with much smaller values of E_p, viz., 9.74, 11.04 and 14.17 kJ/mol. These values indicate that membranes having higher selectivities have higher E_p values due to the hydrophobic silicalite-1 particles present in the membranes.

4.5.3.2. Diffusion coefficient. An increase in diffusion coefficient, D is observed for water in the pristine PVA membrane as compared to pristine NaAlg membrane. Such an increase in D is attributed to the availability of free volume within the membrane matrix. Diffusion coefficients of isopropanol are smaller than water in both PVA and NaAlg membranes, since the permeation of water is predominant compared to isopropanol in both the polymers. Diffusion coefficients of water, isopropanol and water + isopropanol mixtures were calculated from Eq. (6). These data at 30 °C are displayed in Figs. 6 and 7, whereas the bar diagram of diffusion coefficients at higher temperatures (40–60 °C) for 10 wt.% water-containing feed are shown in Fig. 8. Diffusion values increased with increasing temperatures due to the fact that an increase in feed temperature increases thermal mobility of the polymer chains, thereby increasing the diffusion rate.

The temperature dependency of diffusion was also analyzed by a similar type of Arrhenius equation as that of Eq. (22) and diffusion activation parameter, E_D was estimated from the slope of the linear plots of $\ln D$ vs $1/T$ (not displayed) for all the membranes and at all the feed compositions of water + isopropanol feeds. The E_D values of all the membranes are higher than E_p values discussed before. For instance, E_D values of NaAlg, NaAlg-1 and NaAlg-2 membranes are 18.21, 20.36 and 25.2 kJ/mol, respectively, while those for PVA, PVA-1 and PVA-2 membranes are 9.84, 11.14 and 14.3 kJ/mol, respectively. As can be seen from the E_D values, there is an increase in E_D values for high selective membranes, similar to those of E_p values for reasons mentioned before. Using these data, heat of sorption, ΔH_s, values were calculated as:

$$\Delta H_s = E_p - E_D \tag{23}$$

The calculated ΔH_s values for NaAlg, NaAlg-1, NaAlg-2 membranes are −0.06, −0.09 and −0.14 kJ/mol, while for PVA, PVA-1, PVA-2 membranes are −0.1, −0.1 and −0.13 kJ/mol, respectively. Negative values of ΔH_s suggest the exothermic sorption process.

4.5.4. Diffusion and permeation – a comparison between theory and experiment

Experimental and theoretical diffusion coefficients of water, isopropanol and water + isopropanol mixtures at 30 °C are compared in Figs. 6 and 7. As expected, diffusion coefficients of water increase considerably with increasing amount of water in the feed mixture, suggesting that the membranes are water selective. Increase in D values with increasing amount of water in the feed mixture is attributed to the creation of extra free volume in the membrane matrix. Similarly, diffusion coefficients of isopropanol, even though are smaller in magnitude than those observed for water, show the same trend with increasing water in the feed. This trend is also observed for water + isopropanol mixture. As regards the nature of the membranes, diffusion values show a systematic trend for all the membranes. Diffusion generally occurs because of the

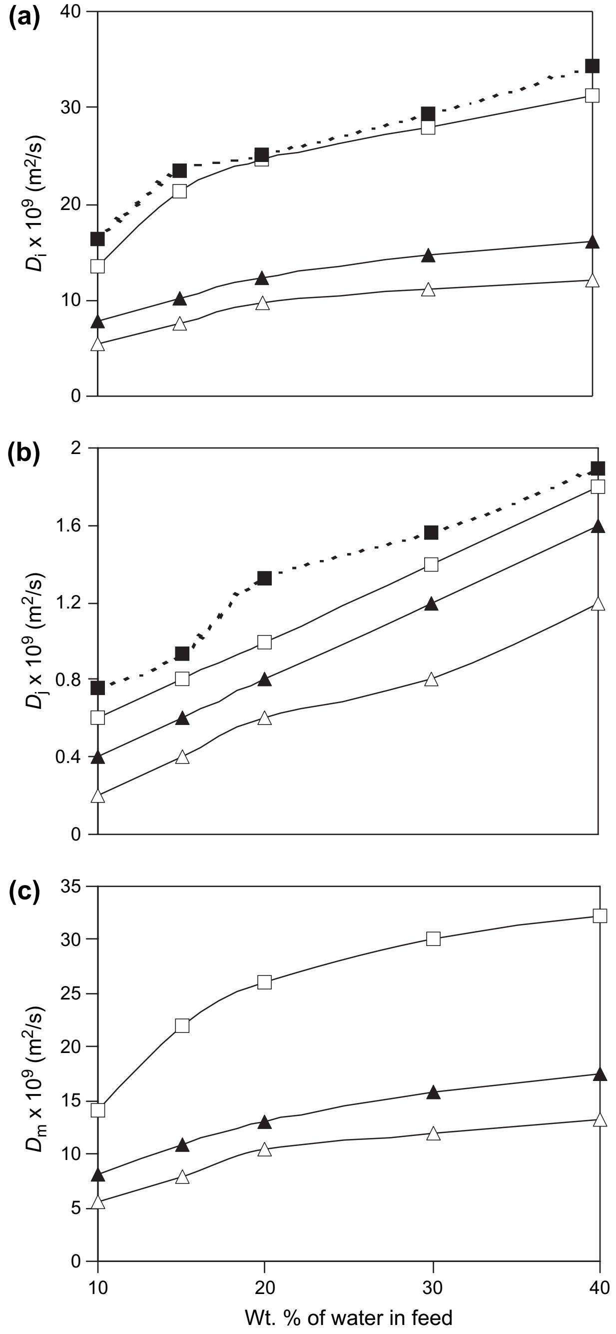

Fig. 6. Diffusion coefficients vs wt.% of water in feed at 30 °C; (---) NaAlg theoretical (■), (—) NaAlg expt. (□), NaAlg-1 (▲) and NaAlg-2 (△) membranes.

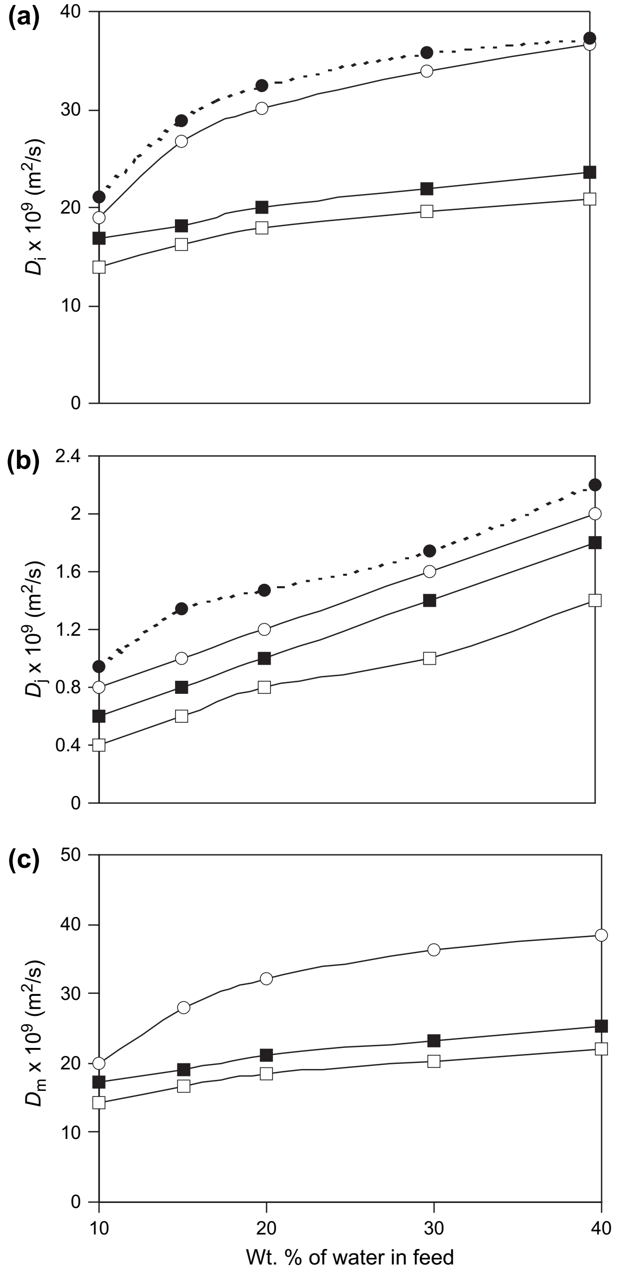

Fig. 7. Diffusion coefficients vs wt.% of water in feed at 30 °C; (---) PVA theoretical (●), (—) PVA expt. (○), PVA-1 (■) and PVA-2 (□) membranes.

presence of a concentration gradient and hence, it is useful to calculate the diffusion coefficient, *D*, of the solvent and solvent mixtures through the membranes from the actual permeation data using Eq. (6). The bar diagram describing pure component diffusion as well as mixed feed media at 40, 50 and 60 °C is displayed in Fig. 8. Due to higher swelling of the membranes at higher temperatures, diffusion coefficients have also increased. From the constructed plots of MSD of water in both PVA and NaAlg polymers as a function of time (in ps) obtained from MD simulations at 30 °C (not displayed here), we found a good agreement with the calculated correlation coefficient values around 0.999 at 95% confidence limit between experimental and simulated data. Experimentally calculated diffusion coefficients systematically decreased from the pristine membranes to the mixed matrix membranes that contained the highest amount of (10 wt.%) silicalite-1 particles. Due to higher swelling of PVA membrane as compared to NaAlg, diffusion coefficients of pristine PVA membrane are also higher than NaAlg membrane. The same trend is observed for mixed matrix membranes of both NaAlg and PVA. As the water content of the feed mixture increases, diffusion coefficients of water and isopropanol also increased due to the plasticization effect.

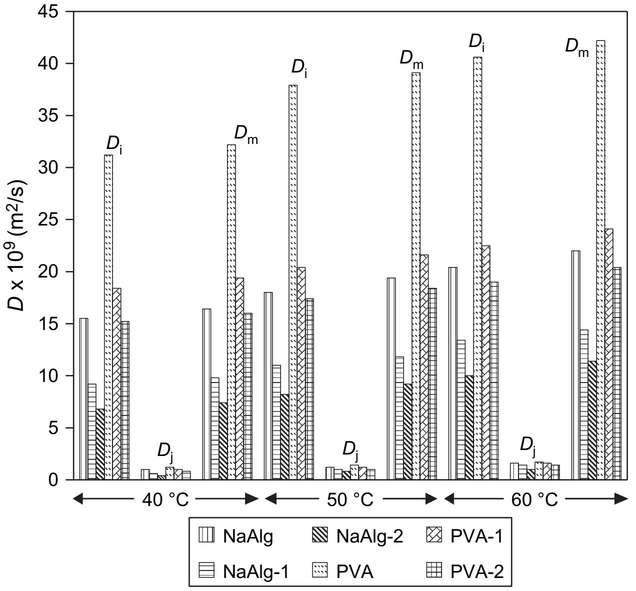

Fig. 8. Bar diagram of diffusion coefficients for higher temperatures at 10 wt.% of water in feed.

Distribution coefficients and permeation coefficients were calculated using Eqs. (7) and (9), respectively. Permeation coefficients, typically displayed in Fig. 9 for NaAlg, showed that permeation coefficients increased with increasing water content of the feed for the obvious reasons discussed in case of diffusion coefficients, but no regular trends were observed for permselectivity as calculated from Eq. (10) because of the difference in the ratio of diffusion coefficients and distribution coefficients between water and isopropanol molecules. A similar trend was also observed for PVA membranes, but these are not displayed graphically. As the feed temperature increased, permeation coefficients of both types of membranes also increased in a manner similar to diffusion coefficients; this is due to the large availability of the number of voids in the mixed matrix membranes at elevated temperatures due to the thermal agitation of polymer chains (see Fig. 10). Permselectivities of the membranes decreased with increasing temperature and these results are in good agreement with selectivities of the membranes. Water flux data calculated from Eq. (12) showed a good agreement with the experimental water flux data at lower water composition of the feed mixture; however, as the feed water composition increased, the calculated flux values decreased as compared to the experimental values (see Fig. 11).

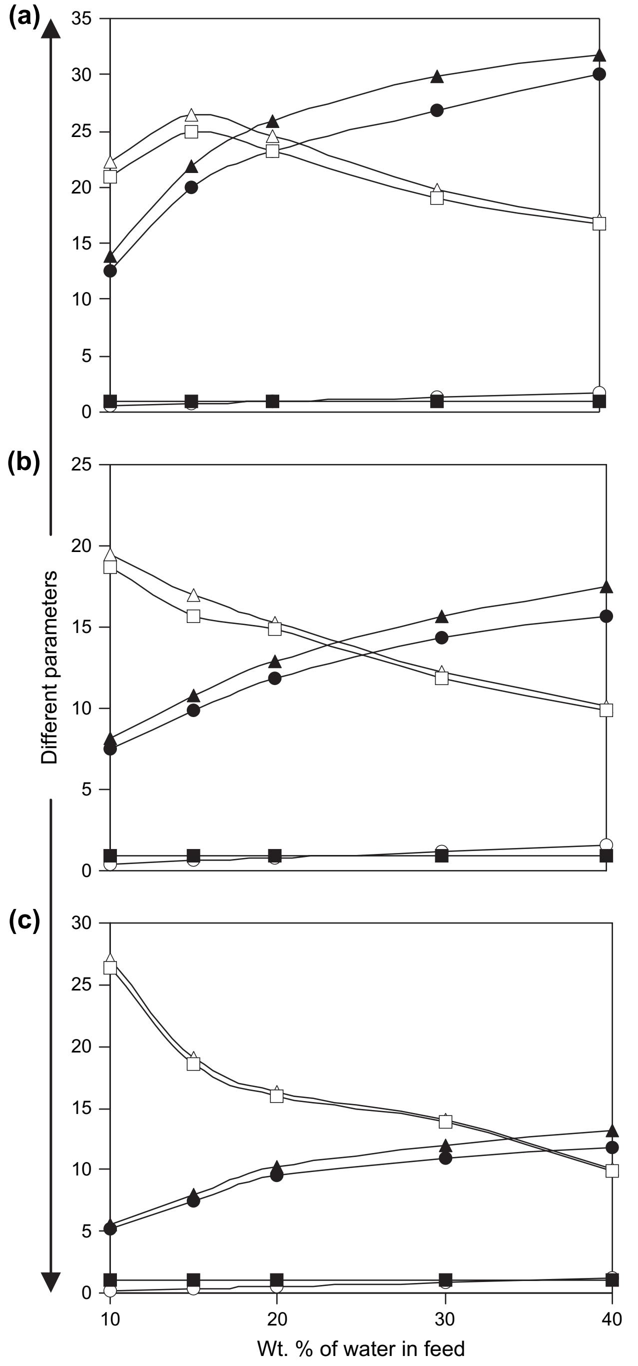

Fig. 9. Different parameters studied with respect to wt.% of water in feed. Symbols: $P_i \times 10^9$ (m^2/s) (●), $P_j \times 10^9$ (m^2/s) (○), $P_m \times 10^9$ (m^2/s) (▲), S_d (△), S_k (■), α_{perm} (□) for (a) NaAlg, (b) NaAlg-1 and (c) NaAlg-2 membranes.

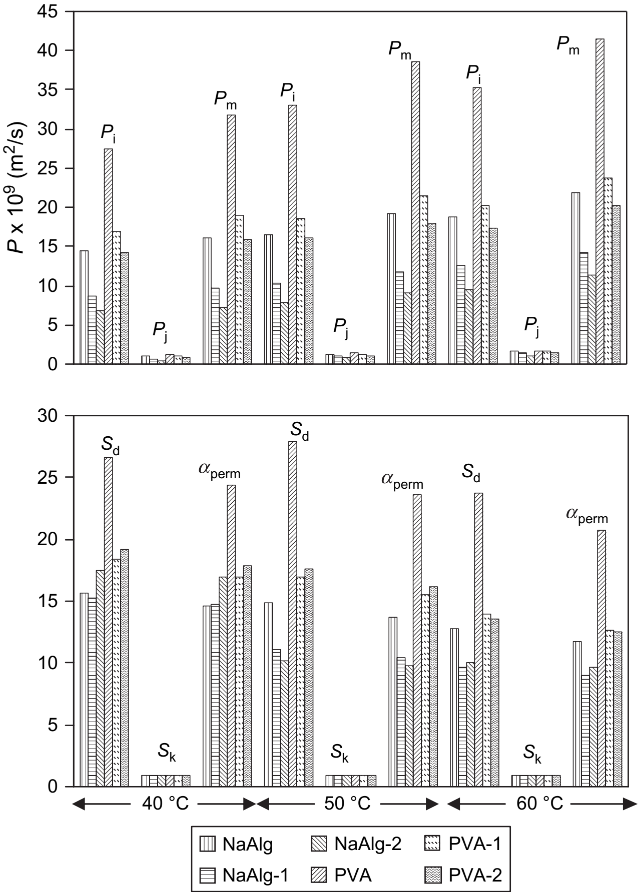

Fig. 10. Bar diagram of different parameters studied for higher temperatures at 10 wt.% of water in feed.

4.6. Silicalite-1 particle interaction with polymers

The surface construction of silicalite-1 is an important step in the calculation of interaction energy. Hence, for silicalite-1, the largest face of the crystal is the (100) surface and this was used as a surface against which NaAlg and PVA came in contact during the simulation step. The pictorial representation of PVA with silicalite-1 is depicted in Fig. 12. The adhesion energy of NaAlg with silicalite-1 is −12.59 kcal/mol, while for PVA, it is smaller, i.e., −1.21 kcal/mol. Thus, in the case of NaAlg, interaction energy is nearly 10 times greater than that of PVA, confirming the greater affinity for silicalite-1 particles. These results follow similar trends as those of PV data. It is noticed that silicalite-1 particles could bind strongly with NaAlg matrix than with PVA matrix, leading to a much higher selectivity for mixed matrix NaAlg membranes than those of the PVA mixed matrix membranes.

4.7. Interaction of NaAlg and PVA with water and isopropanol solvents

Sorption behavior of the chosen polymers with water and isopropanol was estimated using the MD simulation protocols. A representative structure of NaAlg with 10 water molecules is displayed in Fig. 13. Interaction energy values of PVA with water and isopropanol are −31.14 and −25.11 kcal/mol, respectively. In the case of NaAlg, these values are −21.94 and −15.38 kcal/mol, respectively. This suggests that compared to isopropanol, water wets the surface of PVA more than that of NaAlg surface. These values replicate the sorption trends of PVA and NaAlg with water and isopropanol molecules. In any case, the simulated results are quite comparable with the experimental observations.

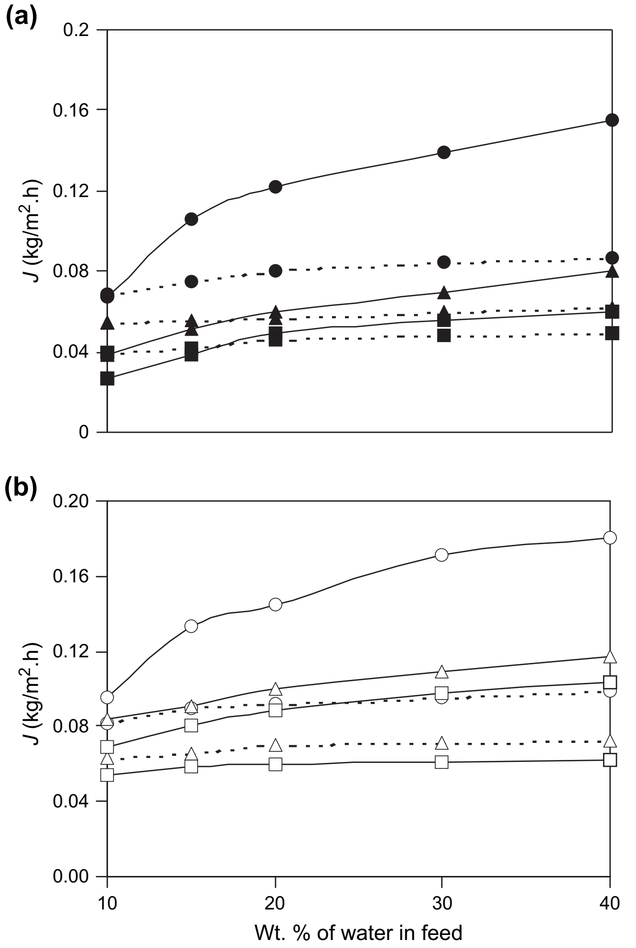

Fig. 11. Flux vs wt.% of water in feed at 30 °C. Symbols: expt. flux (—) and theoretical flux (---) for (a) NaAlg (●), NaAlg-1 (▲), NaAlg-2 (■) and (b) PVA (○), PVA-1 (△), PVA-2 (□) membranes.

4.8. Comparison of PV results with literature data

Incorporation of silicalite-1 into NaAlg or PVA could exert a greater effect on the results of selectivity. Table 2 shows a comparison of the present PV data with literature findings on similar types of membranes. For instance, NaAlg-1, NaAlg-2, PVA-1 and PVA-2 mixed matrix membranes exhibited much higher selectivities than those of the published literature results [15,51–54], but their flux values are lower, due to lower swelling of the polymer after incorporation of hydrophobic silicalite-1 particles.

5. Conclusions

The present study is quite comprehensive to understand sorption, diffusion and permeation trends of the two well-known polymers viz., NaAlg and PVA in pure form as well as their mixed matrix membranes (i.e., after incorporating silicalite-1 particles) to assess their PV performance characteristics. It was observed that 5 and 10 wt.% silicalite-1 loaded NaAlg and PVA mixed matrix membranes were able to successfully dehydrate isopropanol. Incorporation of hydrophobic

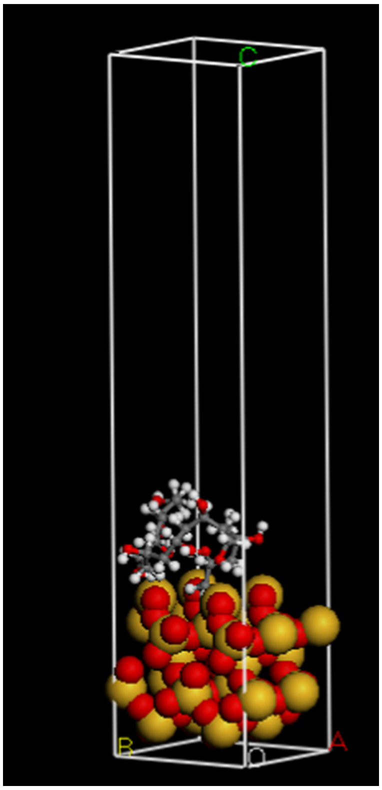

Fig. 12. A typical simulated PVA and its interface with silicalite-1. (carbon atoms are gray, hydrogen — white, oxygen — red). (For interpretation of the references to color in this figure legend, the reader is referred to the web version of this article.)

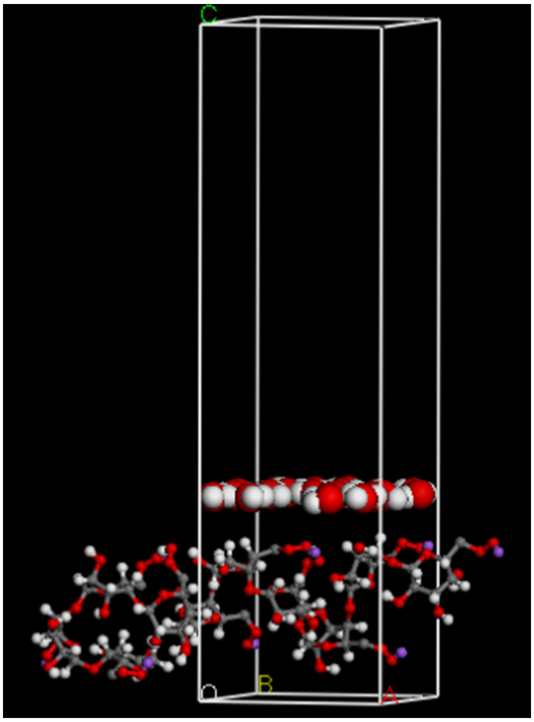

Fig. 13. A representative structure of NaAlg interacting with 10 water molecules. (carbon atoms are gray, hydrogen — white, oxygen — red, sodium — purple). (For interpretation of the references to color in this figure legend, the reader is referred to the web version of this article.)

Table 2
Comparison of PV performance of the present membranes with literature at 30 °C for 10 wt.% water in feed

Membrane type	Water flux (J) ($kg/m^2\,h$)	Selectivity (α)	Ref.
NaAlg-1	0.039	11,241	Present work
NaAlg-2	0.027	17,991	
PVA-1	0.084	1295	Present work
PVA-2	0.069	2241	
NaAlg/PVA (75:25, wt./wt.)	0.125	195	[51]
NaAlg/PVA (50:50, wt./wt.)	0.170	119	
NaAlg/PVA (25:75, wt./wt.)	0.195	91	
PVA/PMMA blend	0.075	400	[52]
Composite membranes of NaAlg and chitosan	0.554	2010	[53]
PVA/KA	0.179	410	[15]
PVA/NaA	0.183	328	
PVA/CaA	0.193	233	
PVA/NaX	0.216	233	
NaAlg + 5% PVA + 10% PEG	0.050	3591	[54]

NaAlg – sodium alginate; PVA – poly(vinyl alcohol); PMMA – poly(methyl methacrylate); KA, NaA, CaA, NaX – zeolites; PEG – poly(ethylene glycol).

silicalite-1 particles has improved the separation characteristics of the mixed matrix membranes over those of pristine NaAlg and PVA membranes with a reduction in swelling. When higher amount (>10 wt.%) of silicalite-1 is embedded into NaAlg and PVA matrices, membranes became brittle and unstable; hence, were not suitable for PV experiments. Tortuous paths created due to the presence of silicalite-1 particles have resulted in higher transport of water molecules than isopropanol. Flux values of the mixed matrix membranes were lower than pristine NaAlg and PVA membranes due to induced hydrophobicity of NaAlg and PVA matrices as a result of the presence of silicalite-1 particles. Diffusion coefficients were higher for water than for isopropanol in pristine as well as both (NaAlg and PVA) the mixed matrix membranes, thus showing their higher water selective nature. Diffusion and permeation coefficients increased as the feed water content and temperature increased, but permselectivity decreased. The computed interaction energy, sorption and diffusion coefficients are in good agreement with the experimental observations. Flory–Huggins theory was successfully employed to predict the sorption selectivities of both the membranes.

Acknowledgements

Authors thank the University Grants Commission (UGC), New Delhi, India for a major funding (F1-41/2001/CPP-II) to establish Center of Excellence in Polymer Science.

References

[1] Aminabhavi TM, Khinnavar RS, Harogoppad SB, Aithal US, Nguyen QT, Hansen KC. J Macromol Sci Rev Macromol Chem Phys 1994;C34:139.
[2] Wang XP. J Membr Sci 2000;170:71.
[3] Kim SG, Lim GT, Jegal J, Lee KH. J Membr Sci 2000;174:1.
[4] Fleming HL, Slater CS. Pervaporation. In: Ho WSW, Sirkar KK, editors. Membrane handbook. New York: van Nostrand Reinhold; 1992.
[5] Yang G, Zhang L, Peng T, Zhong W. J Membr Sci 2000;175:53.
[6] Huang RYM, Yeom CK. J Membr Sci 1991;58:33.
[7] Tsuyumoto M, Karakane H, Maeda Y, Tsgaya H. Desalination 1991;80:139.
[8] Ugarami T, Takigawa K. Polymer 1990;31:668.
[9] Neel J, Nguyen QT, Clement T, Lin DJ. J Membr Sci 1986;27:217.
[10] Lee CH, Hong WH. J Membr Sci 1997;135:187.
[11] Yu J, Lee CH, Hong WH. Chem Eng Process 2002;41:693.
[12] Aminabhavi TM, Naidu BVK, Sridhar S. J Appl Polym Sci 2004;94:1827.
[13] Aminabhavi TM, Naik HG. J Appl Polym Sci 2002;83:273.
[14] Hilmioglu ND, Yildirim AE, Sakaoglu AS, Tulbentci S. Chem Eng Process 2001;40:263.
[15] Gao Z, Yue Y, Li W. Zeolites 1996;16:70.
[16] Chen X, Ping Z, Long Y. J Appl Polym Sci 1998;67:629.
[17] Nomura M, Yamaguchi T, Nakao S. J Membr Sci 1998;144:161.
[18] Boom JR, Print IGM, Zwijnenberg H, de Boer R, Bargeman D, Smolders CA, et al. J Membr Sci 1998;138:237.
[19] Matsuura T. Synthetic membranes and membrane separation processes. Boca Raton: CRC Press; 1994.
[20] Kickelbick G. Prog Polym Sci 2003;28:83.
[21] Prathab B, Subramanian V, Aminabhavi TM. Polymer 2007;48:409.
[22] Accelrys Inc.. MS modeling. San Diego, CA: Accelrys Inc.; 2003.
[23] Eichinger BE, Rigby D, Stein J. Polymer 2002;43:599.
[24] Anjali Devi D, Smitha B, Sridhar S, Aminabhavi TM. J Membr Sci 2005;262:91.
[25] Bhat SD, Aminabhavi TM. Microporous Mesoporous Mater 2006;91:206.
[26] Harogoppad SB, Aminabhavi TM. Macromolecules 1991;24:2598.
[27] Naidu BVK, Aminabhavi TM. Ind Eng Chem Res 2005;44:7481.
[28] Wijmans JG, Baker RW. J Membr Sci 1995;107:1.
[29] Hwang ST, Kammermeyer K. Membranes in separations. New York: Wiley-Interscience; 1975.
[30] Crank J. The mathematics of diffusion. Oxford: Clarendon Press; 1975.
[31] Wijmans JG, Baker RW. J Membr Sci 1993;79:101.
[32] Bell CM, Gerner FL, Strathmann H. J Membr Sci 1988;36:315.
[33] Neto JM, Pinho MN. Sep Purif Technol 2000;18:151.
[34] Aminabhavi TM, Munk P. Macromolecules 1979;12:607.
[35] Mulder MHV, Smolders CA. J Membr Sci 1984;17:289.
[36] Brandrup J, Immergut EH, Grulke EA. Polymer handbook. New York: Wiley-Interscience; 1999.
[37] Aithal US, Aminabhavi TM, Cassidy PE. J Membr Sci 1990;50:225.
[38] Aminabhavi TM, Munk P. J Phys Chem 1980;84:442.
[39] Physical and thermodynamic properties of pure chemicals: evaluated process design data, part 4, 2,2,4-trimethylpentane. Complied by the Design Institute for Physical Property data of the American Institute of Chemical Engineers. Philadelphia: Taylor and Francis; 1999.
[40] Flory PJ. Principles of polymer chemistry. Ithaca, New York: Cornell University Press; 1953.
[41] Sun H. J Phys Chem B 1998;102:7338.
[42] Rigby D, Sun H, Eichinger BE. Polym Int 1997;44:311.
[43] Prathab B, Aminabhavi TM, Parathasarathi R, Manikandan P, Subramanian V. Polymer 2006;47:6914.
[44] Jawalkar SS, Aminabhavi TM. Polym Int 2007;56:928.
[45] Stern SA, Shah VM, Hardy BJ. J Polym Sci Part B Polym Phys 1987;25:1263.
[46] Bowen TC, Noble RD, Falconer JL. J Membr Sci 2004;245:1.
[47] Huang Z, Guan H, Tan WI, Qiao XY, Kulprathipanja S. J Membr Sci 2006;271:223.
[48] Feng X, Huang RYM. Ind Eng Chem Res 1997;36:1048.
[49] Adoor SG, Sairam M, Manjeshwar LS, Raju KVSN. J Membr Sci 2006;285:182.
[50] Fujita H, Kishimoto A, Matsumoto KM. Trans Faraday Soc 1960;56:424.
[51] Kurkuri MD, Aminabhavi TM. J Appl Polym Sci 2003;89:300.
[52] Adoor SG, Manjeshwar LS, Naidu BVK, Sairam M, Aminabhavi TM. J Membr Sci 2006;280:594.
[53] Moon GY, Pal R, Huang YM. J Membr Sci 1999;156:17.
[54] Toti US, Aminabhavi TM. J Membr Sci 2004;228:199.